Interaction and Multiscale Mechanics, Vol. 5, No. 4 (2012) 317-345
DOI: http://dx.doi.org/10.12989/imm.2013.5.4.317

Behavior of cable-stayed bridges under dynamic subsidence of pylons

I.G. Raftoyiannis*, G.T. Michaltsos and T.G. Konstantakopoulos

Department of Civil Engineering, National Technical University of Athens, Greece

(Received September 23, 2012, Revised October 17, 2012, Accepted November 7, 2012)

Abstract. Cable-stayed bridges are often used in modern bridge engineering for connecting two geographical points of long distance. A special load case to cable-stayed bridges is earthquake, which can produce horizontal as well as vertical movements on the pylons of the bridge. These movements may be transient in nature, i.e., only resulting in the transient vibration of the bridge, but causing no damage consequences. In some extreme cases, they may cause permanent subsidence on one or more pylons of the bridge. In this paper, the effect of pylons' subsidence on the dynamic deformations of the bridge and on the cables' strength is thoroughly studied. Conclusions useful to the design of cable-stayed bridges will be drawn from the numerical study.

Keywords: cable-stayed bridges; pylon displacements; fault; pylon dynamic subsidence.

1. Introduction

Cable-stayed bridges have been developed since the beginning of the 18th century as described by Leonard (1972), but they have been of great interest to engineers only in the last 60 years, particularly due to their special shape and also because they constitute an alternative solution to suspension bridges for connecting two geographical points of long distance (Troitsky 1988). The main reasons for their delayed application were difficulties in their static and dynamic analysis, various non-linearities, absence of computational capabilities, as well as lack of high strength materials and construction techniques. Nowadays, numerous studies emerged in the literature concerning the static behavior of cable-stayed bridges, such as the studies by Fleming (1979), Kollbruner *et al*. (1980), Bruno and Grimaldi (1985), Gimsing (1997), Khalil (1999), Virgoreux (1999), Michaltsos *et al*. (2003) and Freire *et al*. (2006). Among the studies concerning the dynamic analysis of cable-stayed bridges are the ones by Fleming and Egeseli (1980), Nazmy and Abdel-Ghaffar (1990), Abdel-Ghaffar and Khalifa (1991), Chatterjee *et al*. (1994), Bruno and Golotti (1994), Achkire and Preumont (1996), Michaltsos (2001), Konstantakopoulos *et al*. (2002), Wang *et al*. (2010) and Mozos and Aparicio (2010). The stability aspects of cable-stayed bridges have also been studied by Ermopoulos *et al*. (1992), Bosdogianni and Olivari (1997), Michaltsos (2005), Michaltsos *et al*. (2008), Michaltsos and Raftoyiannis (2009) and Raftoyiannis *et al.* (2010, 2012).

* Corresponding author, Assistant Professor, E-mail: rafto@central.ntua.gr

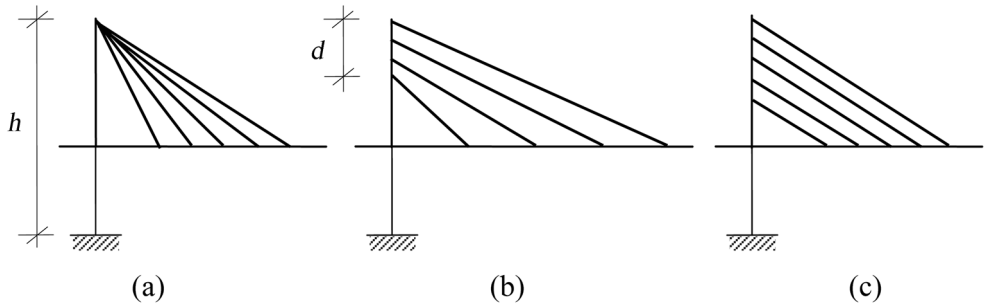

Fig. 1 Cable layout: (a) Fan system, (b) Harp system and (c) Parallel system of cables

In all the above studies, pylon foundation and soil type are two crucial parameters in the design, which have mostly been assumed to be under the normal condition.

A special load case to cable-stayed bridges is earthquake, which can produce horizontal and vertical movements on the pylons of the bridge. These movements may be transient in nature, i.e., only resulting in the transient vibration of the bridge, but causing no damage consequences. In some extreme cases, they may cause permanent subsidence on one or more pylons of the bridge. In this paper, the effect of vertical motion or subsidence of the pylons on the deformations of the bridge and on the cables' strength will be thoroughly studied, using the method introduced for the fan system by Michaltsos *et al*. (2003) and Michaltsos (2005), which is extended herein for the harp system as well. By this method, one can establish the equation that gives the forces of the cables in relation to the deck's deformation, which allows us to convert the problem of cable-stayed bridges to the solution of a continuous beam (i.e., the bridge deck) without cables.

As it is known, the cable layout of a cable-stayed bridge can be divided into three basic types as shown in Fig. 1: the fan system, the harp system and the parallel system of cables. In particular, the parallel system can be regarded as a special case of the harp system. Regarding the harp system of cables, it is a common practice to place the anchorages on the pylons (see Fig. 1(b)) within a short length d usually equal to $h/7$, with h indicating the pylon height, in order to achieve the greatest efficiency of the cables. As a consequence, a harp system of cables is similar to the fan system with height equal to (h-d/2) or (h-d/3).

2. Statement of the problem

Let us consider the bridge in Fig. 2 with the pylons "a" and "b". The bridge is stayed by ρ cables on the left side of pylon "a" and on the right side of pylon "b", and by κ cables on the right of pylon "a" and on the left of pylon "b". Usually, for a harp system, it is assumed $\rho = \kappa$.

Assuming that, when subjected to a seismic action, the pylons move as follows

$$e_a = \alpha_a \sin\Omega_a t$$
$$e_b = \alpha_b \sin\Omega_b (t + \theta) \tag{1a}$$

For the i-th cable on the right-hand side of pylon "a" in Fig. 2, one gets

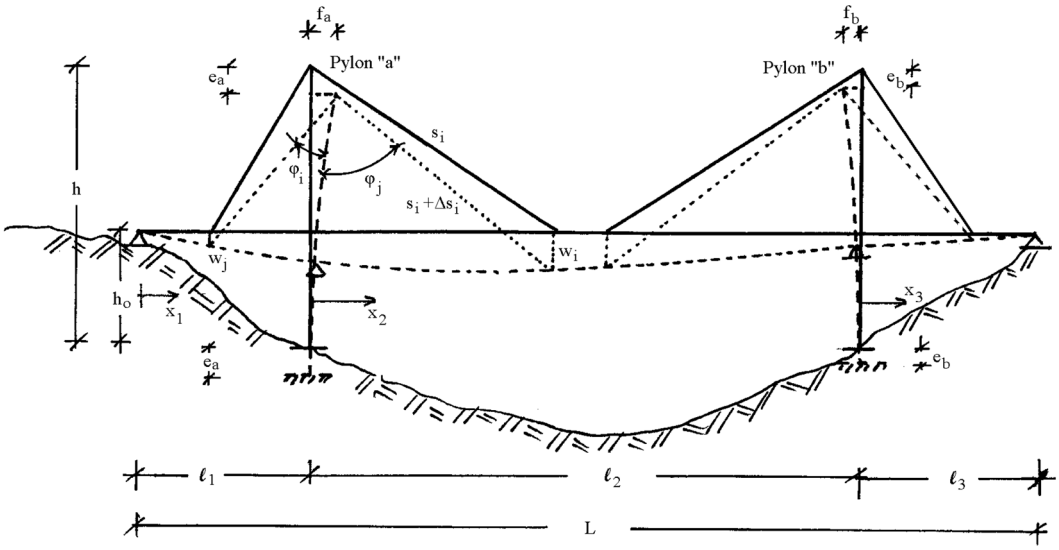

Fig. 2 Relative displacement of two neighboring pylons due to a fault movement

$e_a \cos\varphi_i + f\sin\varphi_i + (s_i + \Delta s_i)\cos\Delta\varphi_i = s_i + w_i\cos\varphi_i$ or because $\cos\Delta\varphi_i \cong 1$ we get

$$\Delta s_i + f\sin\varphi_i + e_a\cos\varphi_i = w_i\cos\varphi_i \tag{1b}$$

By taking into account the relation $\Delta s_i = s_i\, P_i/E_c\, A_i$, Eq. (1b) becomes

$$\frac{s_i\, P_i}{E_c\, A_i} + f\sin\varphi_i = (w_i - e_a)\cos\varphi_i \tag{1c}$$

Similarly, for a cable on the left side of pylon "*a*", one gets

$$\frac{s_j\, P_j}{E_c\, A_j} - f\sin\varphi_j = (w_j - e_a)\cos\varphi_j \tag{1d}$$

3. The fan system

3.1 Pylon's stressing

The deformation $f(z)$ at the point A (z) of the pylon in Fig. 3 is: $E_pI_p(z)f'' = -P_x(z-h)$ or

$$f'(z) = -\int\frac{P_x(z-h)}{E_pI_p}dz + c_1$$

$$f(z) = -\int dz\int\frac{P_x(z-h)}{E_pI_p}dz + c_1z + c_2 \tag{2a}$$

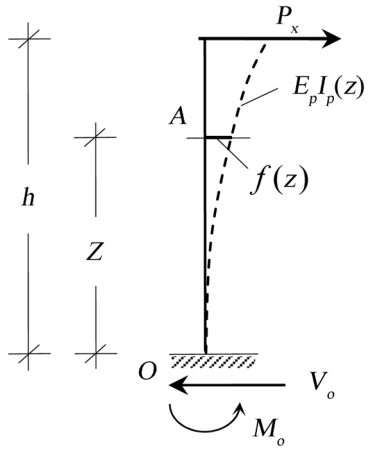

Fig. 3 Deformed configuration of the pylon

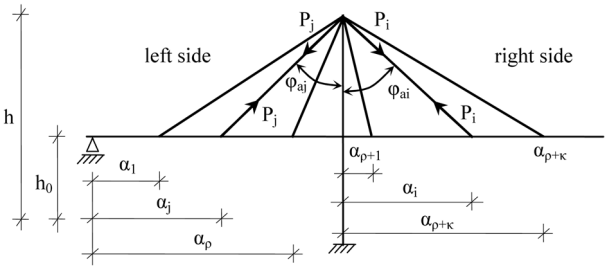

Fig. 4 Forces acting on the pylon due to the cables

With the boundary conditions are: $f(0) = f'(0) = 0$, one obtains from Eq. (2a)

$$f = f_o(z) \cdot P_x \tag{2b}$$

where: $f_o(z) = -\int dz \int \frac{P_x(z-h)}{E_pI_p} dz + \left[\int \frac{P_x(z-h)}{E_pI_p} dz\right]_{z=0} + \left[\int dz \int \frac{P_x(z-h)}{E_pI_p} dz\right]_{z=0}$

For $I_p(z) = I_p = \text{constant}$, it will be $f(z) = -\frac{z^2(z-3h)}{6E_pI_p}$, which for $z = h$ gives

$$f_o = \frac{h^3}{3E_pI_p} \tag{2c}$$

3.2 Relation between P and w

3.2.1 Sparse arrangement of cables

With reference to Fig. 4, the total deformation at the top of the pylon due to the horizontally acting forces is

$$f(h) = f_o(h)\left[\sum_i P_i \sin\varphi_{ai} - \sum_j P_j \sin\varphi_{aj}\right] \tag{3a}$$

Applying Eq. (1b) to both sides of the pylon, one gets

$$\text{left side } \frac{f_o}{b_j}\sin\varphi_{aj}\left(\sum_{j=1}^{\rho} P_j \sin\varphi_{aj} - \sum_{i=1}^{\kappa} P_i \sin\varphi_{ai}\right) + P_j = \frac{\cos\varphi_{aj}}{b_j}(w_j - e_a)$$

$$\text{right side } \frac{f_o}{b_i}\sin\varphi_{ai}\left(\sum_{i=1}^{\kappa} P_i \sin\varphi_{ai} - \sum_{j=1}^{\rho} P_j \sin\varphi_{aj}\right) + P_i = \frac{\cos\varphi_{ai}}{b_i}(w_i - e_a)$$

$$\text{where: } b_j = \frac{s_j}{E_c A_j} \text{ and } b_i = \frac{s_i}{E_c A_i} \tag{3b}$$

Multiplying the first of Eq. (3b) by $\sin\varphi_{aj}$ and adding the ρ equations for the cables considered, and then multiplying the second of Eq. (3b) by $\sin\varphi_{ai}$ and adding the κ equations for the cables considered, one obtains the following relations

$$\text{left side } f_o\sum_{j=1}^{\rho}\frac{\sin^2\varphi_{aj}}{b_j}\left(\sum_{j=1}^{\rho} P_j \sin\varphi_{aj} - \sum_{i=1}^{\kappa} P_i \sin\varphi_{ai}\right) + \sum_{j=1}^{\rho} P_j \sin\varphi_{aj} = \sum_{j=1}^{\rho}\frac{\sin 2\varphi_{aj}}{2b_j}(w_j - e_a)$$

$$\text{right side } f_o\sum_{i=1}^{\kappa}\frac{\sin^2\varphi_{ai}}{b_i}\left(\sum_{i=1}^{\kappa} P_i \sin\varphi_{ai} - \sum_{j=1}^{\rho} P_j \sin\varphi_{aj}\right) + \sum_{i=1}^{\kappa} P_i \sin\varphi_{ai} = \sum_{i=1}^{\kappa}\frac{\sin 2\varphi_{ai}}{2b_i}(w_i - e_a) \tag{3c}$$

Subtracting the above two equations to each other, one finally obtains

$$\Phi_a = \frac{1}{f_o(A_{aj} + A_{ai} + 1)}\left\{\sum_{j=1}^{\rho}\frac{\sin 2\varphi_{aj}}{2b_j}(w_j - e_a) - \sum_{i=1}^{\kappa}\frac{\sin 2\varphi_{ai}}{2b_i}(w_i - e_a)\right\}$$

$$\text{where: } \Phi_a = \sum_{j=1}^{\rho} P_j \sin\varphi_{aj} - \sum_{i=1}^{\kappa} P_i \sin\varphi_{ai}, \quad A_{aj} = \sum_{j=1}^{\rho}\frac{\sin^2\varphi_{aj}}{b_j}, \quad A_{ai} = \sum_{i=1}^{\kappa}\frac{\sin^2\varphi_{ai}}{b_i} \tag{3d}$$

From Eq. (3b), one can easily obtain the cables' stresses as follows

$$P_j = \frac{\cos\varphi_{aj}}{b_j}(w_j - e_a) - f_o\frac{\sin\varphi_{aj}}{b_j}\Phi_a$$

$$P_i = \frac{\cos\varphi_{ai}}{b_i}(w_i - e_a) + f_o\frac{\sin\varphi_{ai}}{b_i}\Phi_a \tag{3e}$$

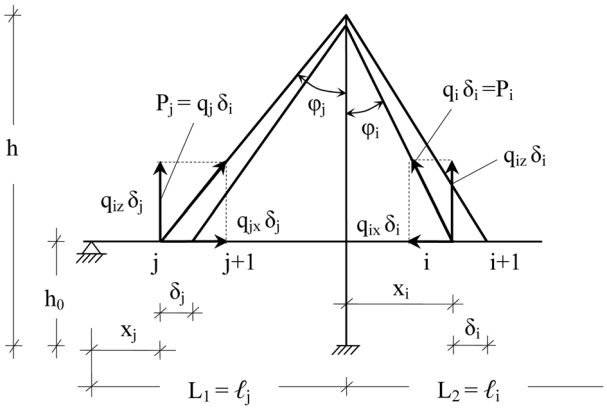

Fig. 5 Pylon force equilibrium under a dense arrangement of cables

3.2.2 Dense arrangement of cables

Let us consider next a dense arrangement of cables in which the distances δ_j and δ_i between two adjacent cables satisfy the following conditions

$$\delta_j \ll \alpha_\rho - \alpha_1 \quad \text{and} \quad \delta_i \ll \alpha_{\rho+\kappa} - \alpha_{\rho+1} \tag{4a}$$

Thus, one may consider a distributed load $q_z(x)$ applied from position α_1 to position α_ρ and from position $\alpha_{\rho+1}$ to position $\alpha_{\rho+\kappa}$, which for position "i" is

$$q_i(x) = \frac{1}{\delta_i} \cdot P_i \tag{4b}$$

Following the notations of Fig. 5, one has

$$s_i = \frac{h-h_o}{\cos\varphi_i}, \quad \sin\varphi_i = \frac{x_i}{\sqrt{(h-h_o)^2 + x_i^2}}, \quad \cos\varphi_i = \frac{h-h_o}{\sqrt{(h-h_o)^2 + x_i^2}}$$

$$s_j = \frac{h-h_o}{\cos\varphi_j}, \quad \sin\varphi_j = \frac{\ell_j - x_j}{\sqrt{(h-h_o)^2 + (\ell_j - x_j)^2}}, \quad \cos\varphi_j = \frac{h-h_o}{\sqrt{(h-h_o)^2 + (\ell_j - x_j)^2}} \tag{4c}$$

and through a process similar to the one of §3.2.1, one obtains for pylon "a"

$$q_{aj}(x) = \frac{\cos\varphi_{aj}}{b_{aj}}(w_j - e_a) - f_o \frac{\sin\varphi_{aj}}{b_{aj}} \Phi_a$$

$$q_{ai}(x) = \frac{\cos\varphi_{ai}}{b_{ai}}(w_i - e_a) + f_o \frac{\sin\varphi_{ai}}{b_{ai}} \Phi_a$$

$$\text{where: } \Phi_a = \frac{1}{f_o(I_{aj} + I_{ai} + 1)} \left[\int_{\alpha 1}^{\alpha\rho} \frac{\sin 2\varphi_{aj}}{2b_{aj}}(w_j - e_a)dx_j - \int_{\alpha(\rho+1)}^{\alpha(\rho+\kappa)} \frac{\sin 2\varphi_{ai}}{2b_{ai}}(w_i - e_a)dx_i \right]$$

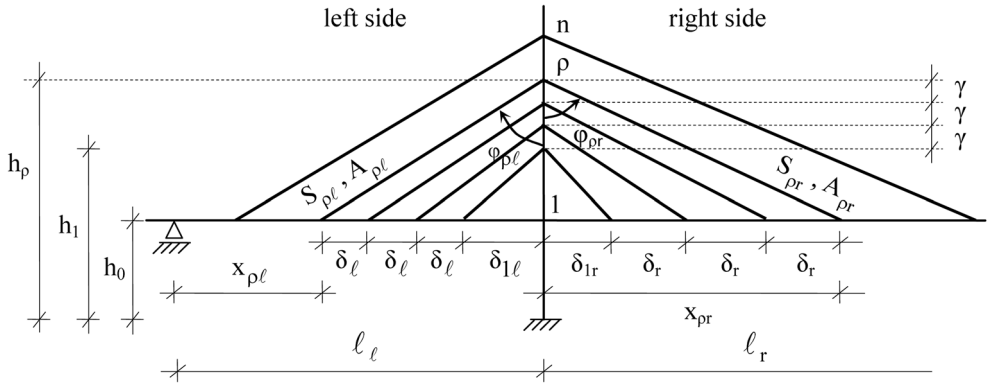

Fig. 6 Cable arrangement in a harp system

$$I_{aj} = \int_{\alpha 1}^{\alpha\rho} \frac{\sin^2\varphi_{aj}}{b_{aj}} dx_j, \quad I_{ai} = \int_{\alpha(\rho+1)}^{\alpha(\rho+\kappa)} \frac{\sin^2\varphi_{ai}}{b_{ai}} dx_i \tag{4d}$$

Similarly, for pylon "*b*" one obtains

$$q_{bj}(x) = \frac{\cos\varphi_{bj}}{b_{bj}}(w_j - e_b) - f_o \frac{\sin\varphi_{bj}}{b_{bj}}\Phi_b$$

$$q_{bi}(x) = \frac{\cos\varphi_{bi}}{b_{bi}}(w_i - e_b) + f_o \frac{\sin\varphi_{bi}}{b_{bi}}\Phi_b + e\frac{\sin\varphi_{bi}}{b_{bi}}$$

$$\text{where: } \Phi_b = \frac{1}{f_o(I_{bj} + I_{bi} + 1)}\left[\int_{b1}^{b\kappa} \frac{\sin 2\varphi_{bj}}{2b_{bj}}(w_j - e_b)dx_j - \int_{b(\kappa+1)}^{b(\kappa+\rho)} \frac{\sin 2\varphi_{bi}}{2b_{bi}}(w_i - e_b)dx_i\right]$$

$$I_{bj} = \int_{b1}^{b\kappa} \frac{\sin^2\varphi_{bj}}{b_{bj}} dx_j, \quad I_{bi} = \int_{b(\kappa+1)}^{b(\kappa+\rho)} \frac{\sin^2\varphi_{bi}}{b_{bi}} dx_i \tag{4e}$$

4. The harp system

The harp system of cables is the most commonly used cable arrangement in bridge engineering (see Fig. 6). It is obvious that the change of the cables' direction should follow a law that will be characteristic for the bridge. The most commonly used law is the one shown in Fig. 6, according to which, the cables are anchored at equal distances γ on the pylon, δ_ℓ on the left side of the deck and δ_r on the right side of the deck. Easily, the following relations can be written

$$\tan\varphi_{\rho\ell} = \frac{\ell_\ell - x_{\rho\ell}}{h_\rho - h_o}, \quad \tan\varphi_{\rho r} = \frac{x_{\rho r}}{h_\rho - h_o}$$

$$s_{\rho\ell} = \frac{\ell_\ell - x_{\rho\ell}}{\sin\varphi_{\rho\ell}}, \quad s_{\rho r} = \frac{x_r}{\sin\varphi_{\rho r}} \tag{5}$$

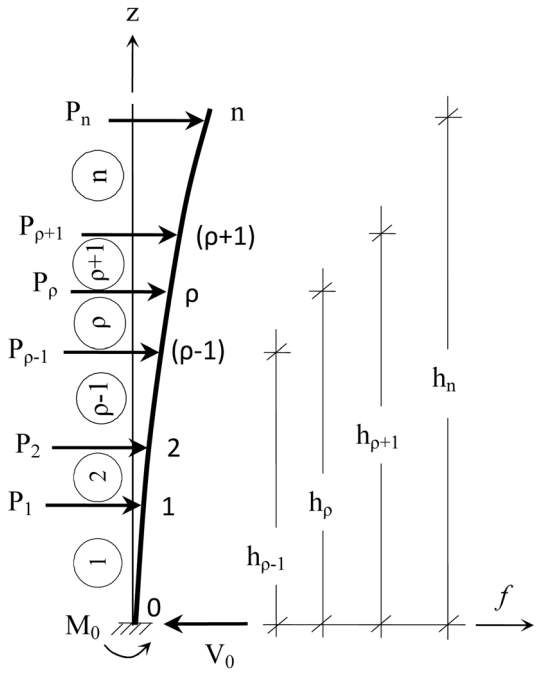

Fig. 7 Pylon stressing due to cables

4.1 Pylon's stressing

The deformation of a pylon subjected to the horizontal forces of the attached cables is shown in Fig. 7. The reactions induced at the end of the pylon are

$$V_o = \sum_1^n P_{x\rho}, \quad M_o = \sum_1^n h_\rho P_{x\rho} \tag{6a}$$

The displacements at each section of the pylon are given by the following relations

$$EI_p f''_{\rho-1} = M_o - zV_o + \sum_1^{\rho-2}(z-h_i)P_{xi} \quad \text{for} \quad z \geq h_{\rho-2}$$

$$EI_p f''_{\rho} = M_o - zV_o + \sum_1^{\rho-1}(z-h_i)P_{xi} \quad \text{for} \quad z \geq h_{\rho-1} \tag{6b}$$

The following continuity conditions must be satisfied

$$f'_{\rho-1}(h_{\rho-1}) = f'_{\rho}(h_{\rho-1}), \quad f_{\rho-1}(h_{\rho-1}) = f_{\rho}(h_{\rho-1}) \tag{6c}$$

Integrating Eq. (6b) one obtains

$$\left.\begin{aligned} EI_p f'_{\rho-1} &= zM_o - \frac{z^2}{2}V_o + \frac{z^2}{2}\sum_1^{\rho-2} P_{xi} - z\sum_1^{\rho-2} h_i P_{xi} + c_{\rho-1} \\ EI_p f'_{\rho} &= zM_o - \frac{z^2}{2}V_o + \frac{z^2}{2}\sum_1^{\rho-1} P_{xi} - z\sum_1^{\rho-1} h_i P_{xi} + c_{\rho} \end{aligned}\right\} \tag{6d}$$

The first condition of Eq. (6c) gives: $c_\rho = c_{\rho-1} + \frac{h_{\rho-1}^2}{2} P_{x(\rho-1)}$. By a similar process, one finally obtains: $c_\rho = c_o + \frac{1}{2}\sum_1^{\rho-1} h_i^2 P_{xi}$. Since, $f'_1(0) = 0$ one gets $c_o = 0$, and thus,

$$c_\rho = \frac{1}{2}\sum_{i=1}^{\rho-1} h_i^2 P_{xi} \tag{6e}$$

Eq. (6d) can be integrated to yield

$$\left.\begin{aligned} EI_p f_{\rho-1} &= \frac{z^2}{2}M_o - \frac{z^3}{6}V_o + \frac{z^3}{6}\sum_1^{\rho-2} P_{xi} - \frac{z^2}{2}\sum_1^{\rho-2} h_i P_{xi} + zc_{\rho-1} + k_{\rho-1} \\ EI_p f_{\rho} &= \frac{z^2}{2}M - \frac{z^3}{6}V_o + \frac{z^3}{6}\sum_1^{\rho-1} P_{xi} - \frac{z^2}{2}\sum_1^{\rho-1} h_i P_{xi} + zc_{\rho} + k_{\rho} \end{aligned}\right\}$$

Introducing the preceding equations into the second equation of Eq. (6c) and following a similar process, one obtains

$$k_\rho = -\frac{1}{6}\sum_{i=1}^{\rho-1} h_i^3 P_{xi} \tag{6f}$$

Thus, the deformation of the pylon can be obtained as follows

$$EI_p f_\rho(z) = -\frac{z^3}{6}\sum_{i=\rho}^{n} P_{xi} + \frac{z^2}{2}\sum_{i=\rho}^{n} h_i P_{xi} + \frac{z}{2}\sum_{i=1}^{\rho-1} h_i^2 P_{xi} - \frac{1}{6}\sum_{i=1}^{\rho-1} h_i^3 P_{xi} \quad \text{for} \quad z \geq h_{\rho-1} \tag{6g}$$

4.2 Relation between P and w

4.2.1 Coarse arrangement of cables

By setting: $a = \frac{1}{EI_p}$, $b_{\rho\ell} = \frac{s_{\rho\ell}}{E_c A_{\rho\ell}}$, $b_{\rho r} = \frac{s_{\rho r}}{E_c A_{\rho r}}$ (7)

applying Eq. (1b) and employing Eq. (6g), one obtains the following relations

$$\text{left side } a\sin^2\varphi_{\rho\ell}\left(\frac{h_\rho^3}{6b_{\rho\ell}}A_o - \frac{h_\rho^2}{2b_{\rho\ell}}A_1 - \frac{h_\rho}{2b_{\rho\ell}}A_2 + \frac{1}{6b_{\rho\ell}}A_3\right) + P_{x\rho\ell} = \frac{(w_{\rho\ell} - e_a)}{2b_{\rho\ell}}\sin 2\varphi_{\rho\ell}$$

$$\text{right side } a\sin^2\ \varphi_{\rho r}\left(-\frac{h_\rho^3}{6b_{\rho r}}A_o+\frac{h_\rho^2}{2b_{\rho r}}A_1+\frac{h_\rho}{2b_{\rho r}}A_2-\frac{1}{6b_{\rho r}}A_3\right)+P_{x\rho r}\ =\ \frac{(w_{\rho r}-e_a)}{2b_{\rho r}}\sin 2\varphi_{\rho r} \tag{8a}$$

where:

$$A_o\ =\ \sum_{i=\rho}^{n}(P_{xir}-P_{xi\ell})$$

$$A_1\ =\ \sum_{i=\rho}^{n}h_i(P_{xir}-P_{xi\ell})$$

$$A_2\ =\ \sum_{i=1}^{\rho-1}h_i^2(P_{xir}-P_{xi\ell})$$

$$A_3\ =\ \sum_{i=1}^{\rho-1}h_i^3(P_{xir}-P_{xi\ell}) \tag{8b}$$

By repeating the first line of Eq. (8a) from ρ to n and adding the results, then by repeating the second line of Eq. (8a) also from ρ to n and adding the results as well, one obtains two equations which can be subtracted from each other to yield

$$\left(-\frac{a}{6}Q_3+1\right)A_o+\frac{a}{2}Q_2A_1+\frac{a}{2}Q_1A_2-\frac{a}{6}Q_oA_3\ =\ S_o+F_o \tag{9a}$$

By multiplying the first line of Eq. (8a) by h_ρ, repeating the results from ρ to n and adding the obtained expressions, then by performing the same procedure for the second line of Eq. (8a), and finally by subtracting the two results, one obtains

$$-\frac{a}{6}Q_4A_o+\left(\frac{a}{2}Q_3+1\right)A_1+\frac{a}{2}Q_2A_2-\frac{a}{6}Q_1A_3\ =\ S_1+F_1 \tag{9b}$$

Following the same procedure, but multiplying firstly by h_ρ^2 and then by h_ρ^3 and repeating the outcome from 1 to $\rho-1$, one obtains the following equations

$$\left.\begin{aligned}-\frac{a}{6}R_5A_o+\frac{a}{2}R_4A_1+\left(\frac{a}{2}R_3+1\right)A_2-\frac{a}{6}R_2A_3\ &=\ T_2+D_2\\ -\frac{a}{6}R_6A_o+\frac{a}{2}R_5A_1+\frac{a}{2}R_4A_2+\left(-\frac{a}{6}R_3+1\right)A_3\ &=\ T_3+D_3\end{aligned}\right\} \tag{9c,d}$$

where:

$$Q_m\ =\ \sum_{i=\rho}^{n}\frac{h_i^m}{b_{ir}}\sin^2\varphi_{ir}+\sum_{i=\rho}^{n}\frac{h_i^m}{b_{i\ell}}\sin^2\varphi_{i\ell}$$

$$R_m\ =\ \sum_{i=1}^{\rho-1}\frac{h_i^m}{b_{ir}}\sin^2\varphi_{ir}+\sum_{i=1}^{\rho-1}\frac{h_i^m}{b_{i\ell}}\sin^2\varphi_{i\ell}$$

$$S_m = \sum_{i=\rho}^{n} \frac{h_i^m}{2b_{ir}} \sin 2\varphi_{ir} w_{ir} - \sum_{i=\rho}^{n} \frac{h_i^m}{2b_{i\ell}} \sin 2\varphi_{i\ell} w_{i\ell}$$

$$T_m = \sum_{i=1}^{\rho-1} \frac{h_i^m}{2b_{ir}} \sin 2\varphi_{ir} w_{ir} - \sum_{i=1}^{\rho-1} \frac{h_i^m}{2b_{i\ell}} \sin 2\varphi_{i\ell} w_{i\ell}$$

$$F_m = e\sum_{i=\rho}^{n} \frac{h_i^m}{b_{ir}} \sin^2 \varphi_{ir} + e\sum_{i=\rho}^{n} \frac{h_i^m}{b_{i\ell}} \sin^2 \varphi_{i\ell}$$

$$D_m = e\sum_{i=1}^{\rho-1} \frac{h_i^m}{b_{ir}} \sin^2 \varphi_{ir} + e\sum_{i=1}^{\rho-1} \frac{h_i^m}{b_{i\ell}} \sin^2 \varphi_{i\ell} \tag{9e}$$

From the system of Eqs. (9a) to (9d), one obtains the terms A_o, A_1, A_2, A_3 and from Eq. (8a) one obtains the stresses of the cables, which are

$$P_{\rho\ell} = \frac{\cos\varphi_{\rho\ell}}{b_{\rho\ell}}(w_{\rho\ell} - e_a) - a\left(\frac{h_\rho^3}{6b_{\rho\ell}}A_o - \frac{h_\rho^2}{2b_{\rho\ell}}A_1 - \frac{h_\rho^2}{2b_{\rho\ell}}A_2 + \frac{h_\rho^3}{6b_{\rho\ell}}A_3\right)$$

$$P_{\rho r} = \frac{\cos\varphi_{\rho r}}{b_{\rho r}}(w_{\rho r} - e_a) + a\left(\frac{h_\rho^3}{6b_{\rho r}}A_o - \frac{h_\rho^2}{2b_{\rho r}}A_1 - \frac{h_\rho^2}{2b_{\rho r}}A_2 + \frac{h_\rho^3}{6b_{\rho r}}A_3\right) \tag{9f}$$

4.2.2 Dense arrangement of cables

Let us consider next a dense arrangement of cables, as shown in Fig. 8. Assume that the distances δ_r and δ_ℓ between two adjacent cables satisfy the conditions

$$\delta_\ell \ll \alpha_n - \alpha_1 \quad \text{and} \quad \delta_r \ll \alpha_{2n} - \alpha_{n+1} \tag{10a}$$

For this case, we consider a distributed load $q_z(x)$ applied from position α_1 to position α_n and from position α_{n+1} to position α_{2n}, which at position x_r are

$$q_{zr}(x_r) = \frac{1}{\delta_r} P_{\rho r} \cos\varphi_{\rho r} \tag{10b}$$

Following the notations of Fig. 8, Eq. (5) become

$$\tan\varphi_\ell = \frac{\ell_\ell - x_\ell}{h_\rho - h_o}, \quad \tan\varphi_r = \frac{x_r}{h_\rho - h_o}$$

$$s_\ell = \frac{\ell_\ell - x_\ell}{\sin\varphi_\ell}, \quad s_\ell = \frac{x_r}{\sin\varphi_r} \tag{11}$$

Eq. (7) can be written as follows

$$a = \frac{1}{EI_p}, \quad b_\ell = \frac{\ell_\ell - x_\ell}{E_c A_c \sin\varphi_\ell}, \quad b_r = \frac{x_r}{E_c A_c \sin\varphi_r} \tag{12}$$

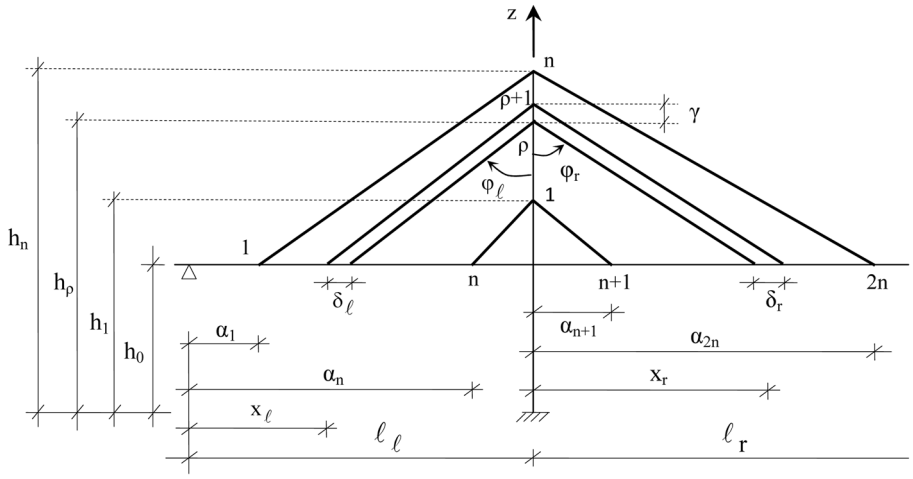

Fig. 8 Harp system of cables with dense arrangement

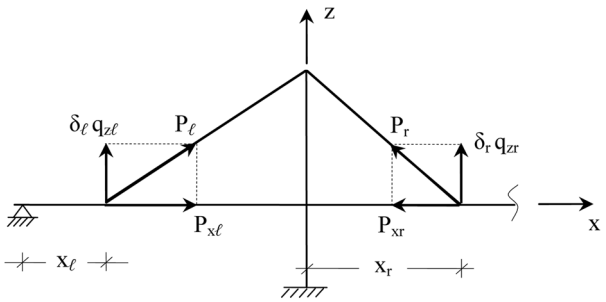

Fig. 9 Pylon stressing due to a dense arrangement of cables

One can express x_ℓ and x_r with respect to coordinate z as follows: $\rho = \dfrac{z-h_1}{\gamma}$, $x_\ell = \alpha_n - \rho\delta_\ell$, and $x_r = \alpha_{n+1} + \rho\delta_r$, or finally

$$x_\ell = \alpha_n - \frac{z-h_1}{\gamma}\delta_\ell, \quad x_r = \alpha_{n+1} + \frac{z-h_1}{\gamma}\delta_r \tag{13}$$

In addition, from Eq. (10) one can write the following based on Fig. 9

$$P_{xr} = P_r \sin\varphi_r = \delta_r q_{zr} \tan\varphi_r, \quad P_{x\ell} = P_\ell \sin\varphi_\ell = \delta_\ell q_{z\ell} \tan\varphi_\ell \tag{14}$$

Then, Eq. (8b) can be written as follows

$$\bar{A}_o = \int_z^{h_n} (P_{xr} - P_{x\ell}) dx$$

$$\overline{A}_1 = \int_z^{h_n} z(P_{xr} - P_{x\ell})dx$$

$$\overline{A}_2 = \int_{h_1}^{z} z^2(P_{xr} - P_{x\ell})dx$$

$$\overline{A}_3 = \int_{h_1}^{z} z^3(P_{xr} - P_{x\ell})dx \tag{15a}$$

and the system of Eqs. (9a) to (9d) becomes

$$\left(-\frac{a}{6}\overline{Q}_3 + 1\right)\overline{A}_o + \frac{a}{2}\overline{Q}_2\overline{A}_1 + \frac{a}{2}\overline{Q}_1\overline{A}_2 - \frac{a}{6}\overline{Q}_o\overline{A}_3 = \overline{S}_o + \overline{F}$$

$$-\frac{a}{6}\overline{Q}_4\overline{A}_o + \left(\frac{a}{2}\overline{Q}_3 + 1\right)\overline{A}_1 + \frac{a}{2}\overline{Q}_2\overline{A}_2 - \frac{a}{6}\overline{Q}_1\overline{A}_3 = \overline{S}_1 + \overline{F}_1$$

$$-\frac{a}{6}\overline{R}_5\overline{A}_o + \frac{a}{2}\overline{R}_4\overline{A}_1 + \left(\frac{a}{2}\overline{R}_3 + 1\right)\overline{A}_2 - \frac{a}{6}\overline{R}_2\overline{A}_3 = \overline{T}_2 + \overline{D}_2$$

$$-\frac{a}{6}\overline{R}_6\overline{A}_o + \frac{a}{2}\overline{R}_5\overline{A}_1 + \frac{a}{2}\overline{R}_4\overline{A}_2 + \left(-\frac{a}{6}\overline{R}_3 + 1\right)\overline{A}_3 = \overline{T}_3 + \overline{D}_3 \tag{15b}$$

where:

$$\overline{Q}_m = \int_z^h \frac{z^m}{b_r}\sin^2\varphi_r dz + \int_z^h \frac{z^m}{b_\ell}\sin^2\varphi_\ell dz$$

$$\overline{R}_m = \int_{h_1}^z \frac{z^m}{b_r}\sin^2\varphi_r dz + \int_{h_1}^z \frac{z^m}{b_\ell}\sin^2\varphi_\ell dz$$

$$\overline{S}_m = \int_z^h \frac{z^m}{2b_r}\sin 2\varphi_r w_r dz - \int_z^h \frac{z^m}{2b_\ell}\sin 2\varphi_\ell w_\ell dz$$

$$\overline{T}_m = \int_{h_1}^z \frac{z^m}{2b_r}\sin 2\varphi_r w_r dz - \int_{h_1}^z \frac{z^m}{2b_\ell}\sin 2\varphi_\ell w_\ell dz$$

$$\overline{F}_m = e\overline{Q}_m$$

$$\overline{D}_m = e\overline{R}_m \tag{15c}$$

By solving the above system of equations, the coefficients $\overline{A}_o, \overline{A}_1, \overline{A}_2$ and $\overline{A}_3$ are determined. Consequently, the stresses of the cables can be determined as follows

$$q_{z\ell}(x_\ell) = \frac{\cos\varphi_\ell}{b_\ell}(w_\ell - e_a) - \frac{a\sin\varphi_\ell}{b_\ell}\left(\frac{z^3}{6}\overline{A}_o - \frac{z^2}{2}\overline{A}_1 - \frac{z}{2}\overline{A}_2 + \frac{1}{6}\overline{A}_3\right)$$

$$q_{zr}(x_r) = \frac{\cos\varphi_r}{b_r}(w_r - e_a) + \frac{a\sin\varphi_r}{b_r}\left(\frac{z^3}{6}\overline{A}_o - \frac{z^2}{2}\overline{A}_1 - \frac{z}{2}\overline{A}_2 + \frac{1}{6}\overline{A}_3\right) \tag{15d}$$

5. The deformations of the deck

The deformations of a bridge deck subjected to the vertical movements $e_a = e_a(t)$ and $e_b = e_b(t)$ of the pylons "*a*" and "*b*" supports as shown in Fig. 2 due to earthquake, can be given as follows based on the relation

$$w(x, t) = w_s(x, t) + w_o(x, t) = g_a(x) \cdot e_a(t) + g_b(x) \cdot e_b(t) + w_o(x, t) \tag{16}$$

where w_s is the movement of the bridge deck (beam) as an undeformed body, and w_o is the elastic deformation of the bridge deck as elastic beam. In addition, $g_1(x)$ and $g_2(x)$ are the influence functions of a simply supported beam (or of a three-span continuous beam). The equation governing the motion of the bridge deck is

$$E_b I_b w'''' + c_b\dot{w} + m_b\ddot{w} = g(x) + p(x) + \sum_{\varphi} P_\varphi \delta(x - x_\varphi) - q(x, w) \tag{17}$$

where E_b is the modulus of elasticity of the bridge deck,
I_b is the moment of inertia of the cross-section of the bridge-deck,
c_b is the damping coefficient of the bridge-deck,
m_b is the mass per unit length of the deck,
$w(x)$ is the total vertical displacement of the deck and
$g(x)$ is the dead load of the bridge,
$p(x)$ is the live load
P_φ are concentrated loads (dead or live) at positions $x = x_\varphi$
$q(x, w)$ are the forces due to the cables and
$\delta(x)$ is the Dirac-delta function.

By the use of Eq. (17), Eq. (16) becomes

$$E_b I_b w_o'''' + c_b\dot{w}_o + m_b\ddot{w}_o = -m\ddot{F}(x, t) - c\dot{F}(x, t) + g(x) + p(x) + \sum_{\varphi} P_\varphi \delta(x - x_\varphi) - q(x, w) \tag{18}$$

where: $F(x, t) = g_a(x) \cdot e_a(t) + g_b(x) \cdot e_b(t)$

Here, one is searching a solution of the form

$$w_o = \sum_n Z_n(x) T_n(t) \tag{19}$$

where $T_n(t)$ are the unknown time functions (under determination) and $Z_n(x)$ are arbitrarily chosen functions of x that satisfy the boundary conditions of the deck. In this case, the shape functions of the corresponding continuous beam, which has the same characteristics as the bridge deck, but without cables, are chosen. Substituting Eq. (19) into Eq. (18), one gets

$$E_b I_b \sum_n Z X_n'' T_n + c_b \sum_n Z_n \dot{T}_n + m \sum_n Z_n \ddot{T}_n = g(x) + p(x) + \sum_\varphi P_\varphi \delta(x - x_\varphi) - q\left(x, \left[w_s + \sum_n Z_n T_n\right]\right) \quad (20a)$$

Remember that Z_n satisfies the equation of the free motion of a beam, which has the same characteristics as the bridge deck but without cables. By multiplying the preceding equation by Z_ρ, integrating the outcome, and taking into account the orthogonality conditions, one obtains the following equation

$$\ddot{T}_\rho + 2\beta\dot{T}_\rho + \omega_\rho^2 T_\rho = \Gamma_\rho \left[\int_0^L [-\ddot{F} - 2\beta\dot{F} + g + p(x)] Z_\rho dx - \int_0^L q\left(x, \left(w_s + \sum_n Z_n T_n\right)\right) Z_\rho dx \right] \quad (20b)$$

where: $\beta = \dfrac{c_b}{2m}$ and $\Gamma_\rho = \dfrac{1}{m \int_0^L Z_\rho^2 dx}$

Here ω_ρ are the eigenfrequencies of the beam, which has the same characteristics as the bridge deck but without cables. Eq. (20b) can be written in the following form

$$\ddot{T}_\rho + 2\beta\dot{T}_\rho + \omega_\rho^2 T_\rho = C_{\rho 1} T_1 + C_{\rho 2} T_2 + \ldots + C_{\rho n} T_n + R_\rho \quad (20c)$$

with $\rho = 1$ to n

where:

$$C_{\rho k} = -\Gamma_k \left(\int_0^{\ell_1} A_{aj} Z_{ak}^2 dx_1 + \int_0^{\ell_2} (A_{ai} + A_{bj}) Z_{bk}^2 dx_2 + \int_0^{\ell_3} A_{bi} Z_{ck}^2 dx_3 \right)$$

$$-\Gamma_k \left\{ -F_a \cdot \left(\int_{\alpha_1}^{\alpha_\rho} B_{aj} Z_{ak} dx_1 - \int_{\alpha_{\rho+1}}^{\alpha_{\rho+k}} B_{ai} Z_{bk} dx_2 \right) \left(\int_0^{\ell_1} A_{aj} Z_{ak} dx_1 - \int_0^{\ell_2} A_{ai} Z_{bk} dx_2 \right) \right.$$

$$\left. -F_b \cdot \left(\int_{b_1}^{b_k} B_{bj} Z_{bk} dx_2 - \int_{b_{k+1}}^{b_{k+\rho}} B_{bi} Z_{ck} dx_3 \right) \left(\int_0^{\ell_2} A_{bj} Z_{bk} dx_2 - \int_0^{\ell_3} A_{bi} Z_{ck} dx_3 \right) \right\} \quad (20d)$$

$$R_\rho = \Gamma_\rho \left(g \int_0^L Z_\rho dx + \int_0^L p(x) Z_\rho dx \right)$$

$$-\Gamma_\rho \left(\int_0^{\ell_1} g_{a1} Z_{a\rho} dx_1 + \int_0^{\ell_2} g_{a2} Z_{b\rho} dx_2 + \int_0^{\ell_3} g_{a3} Z_{c\rho} dx_3 \right) (\ddot{e}_a + 2\beta\dot{e}_a)$$

$$-\Gamma_\rho \left(\int_0^{\ell_1} g_{a1} Z_{a\rho} dx_1 + \int_0^{\ell_2} g_{a2} Z_{b\rho} dx_2 + \int_0^{\ell_3} g_{a3} Z_{c\rho} dx_3 \right) (\ddot{e}_a + 2\beta\dot{e}_a)$$

$$-\Gamma_\rho\left(\int_0^{\ell_1} A_{aj}g_{a1}Z_{a\rho}dx_1+\int_0^{\ell_2}(A_{ai}+A_{bj})g_{a2}Z_{b\rho}dx_2+\int_0^{\ell_3}A_{bi}g_{a3}Z_{c\rho}dx_3\right)\cdot e_a$$

$$-\Gamma_\rho\left(\int_0^{\ell_1} A_{aj}g_{b1}Z_{a\rho}dx_1+\int_0^{\ell_2}(A_{ai}+A_{bj})g_{b2}Z_{b\rho}dx_2+\int_0^{\ell_3}A_{bi}g_{b3}Z_{c\rho}dx_3\right)\cdot e_b$$

$$-\Gamma_\rho\left\{-F_a\left(\int_{a_1}^{a_\rho}B_{aj}(g_{a1}e_a+g_{b1}e_b-e_a)dx_1-\int_{a_{\rho+1}}^{a_{\rho+k}}B_{ai}(g_{a2}e_a+g_{b2}e_b-e_a)dx_2\right)\left(\int_0^{\ell_1}A_{aj}Z_{a\rho}dx_1-\int_0^{\ell_2}A_{ai}Z_{b\rho}dx_2\right)\right.$$

$$\left.-F_b\left(\int_{b_1}^{b_k}B_{bj}(g_{a2}e_a+g_{b2}e_b-e_b)dx_2-\int_{b_{k+1}}^{b_{k+\rho}}B_{bi}(g_{a3}e_a+g_{b3}e_b-e_b)dx_3\right)\left(\int_0^{\ell_2}A_{bj}Z_{b\rho}dx_2-\int_0^{\ell_3}A_{bi}Z_{c\rho}dx_3\right)\right\} \tag{20e}$$

and:

$$A_{aj}=\frac{\cos\varphi_{aj}}{b_{aj}},\quad A_{ai}=\frac{\cos\varphi_{ai}}{b_{ai}},\quad A_{bj}=\frac{\cos\varphi_{bj}}{b_{bj}},\quad A_{bi}=\frac{\cos\varphi_{bi}}{b_{bi}}$$

$$B_{aj}=\frac{\sin 2\varphi_{aj}}{2b_{aj}},\quad B_{ai}=\frac{\sin 2\varphi_{ai}}{2b_{ai}},\quad B_{bj}=\frac{\sin 2\varphi_{bj}}{2b_{bj}},\quad B_{bi}=\frac{\sin 2\varphi_{bi}}{2b_{bi}}$$

$$F_a=\frac{f_o}{f_o(I_{aj}+I_{ai})+1},\quad F_b=\frac{f_o}{f_o(I_{bj}+I_{bi})+1} \tag{20f}$$

In order to solve Eq. (20c), one applies Laplace's transformation. To this end, one sets

$$LT_\rho(t)=S_\rho(s)$$
$$LR_\rho(t)=\Phi_\rho(s) \tag{21a}$$

and with the initial conditions $T_\rho(0)=\dot{T}_\rho(0)=0$, one gets

$$L\dot{T}_\rho(t)=s\cdot S_\rho(s)$$
$$L\ddot{T}_\rho(t)=s^2\cdot S_\rho(s) \tag{21b}$$

Therefore, Eq. (20b) becomes

$$C_{\rho1}S_1+C_{\rho2}S_2+\ldots+(s^2+2\beta s+\omega_\rho^2+C_{\rho\rho})S_\rho+\ldots+C_{\rho n}S_n=-\Phi_\rho \tag{21c}$$

with: $\rho=1$ to n

Solving the preceding linear system of equations, one finally finds

$$S_\rho=\frac{N_\rho(s)}{M_\rho(s)} \tag{21d}$$

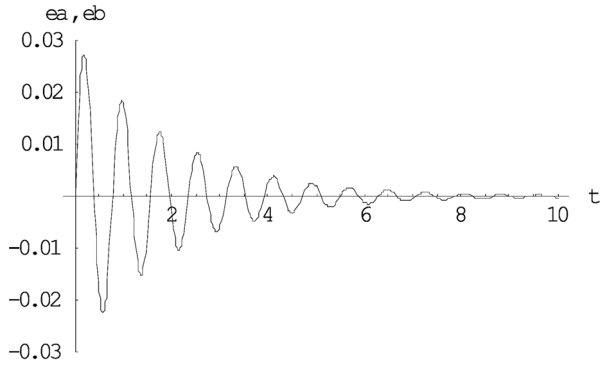

Fig. 10 Oscillation of both pylons

with M_ρ of higher degree than the polynomial N_ρ. Thus one can apply the Heaviside rule to obtain

$$T_\rho(t) = L^{-1}S_\rho(s) \tag{21e}$$

Therefore,

$$w(x,t) = w_s(x,t) + w_o(x,t) = g_a(x)e_a(t) + g_b(x)e_b(t) + \sum_n Z_n T_n \tag{21f}$$

6. Numerical results and discussion

In order to study the influence of the dynamic subsidence of the pylons on the deck deformation and on the cables stresses, one considers a cable-stayed bridge of the fan system with two kinds of pylons, i.e., one with slender pylons of $I_p = 100*I_b$ and the other with stiff pylons of $I_p = 1000*I_b$. The characteristics of the bridge are

$L_1 = L_3 = 250$ m, $L2 = 480$ m, $h_o = 130$ m, $h = 240$ m, $\alpha_1 = 20$ m, $\alpha_n = 240$ m, $\alpha_{n+1} = 60$ m,

$\alpha_{n+k} = 230$ m, $b_1 = 250$ m, $b_k = 420$ m, $b_{k+1} = 10$ m, $b_{k+n} = 230$ m, $\delta_1 = 8.8$ m, $\delta_r = 9.6$ m,

$m = 1000$ kg/m, $g = 10000$ dN / m, $I_b = 1.4$ m^4, $Eb = Ec = 2.1 \cdot 10^{10}$ dN / m^2

The eigenfrequencies of the bridge-deck, as a three-span beam without cables are

$$\omega_1 = 0.358726 \text{ sec}^{-1},\ \omega_2 = 0.889219 \text{ sec}^{-1},\ \omega_3 = 1.09658 \text{ sec}^{-1},\ \omega_4 = 3.20926 \text{ sec}^{-1}$$

while for the shape functions of the above beam and the influence functions $g_1(x)$ and $g_2(x)$ see Michaltsos and Raftoyiannis (2012).

6.1 Both pylons with the same oscillation

Let us consider that both pylons oscillate according to the following equation

$$e_a = e_b = 0.03 \cdot e^{-0.5 \cdot t}\text{Sin}(8 \cdot t) \tag{22}$$

as shown in Fig. 10. By applying the formulae of §4 and 5, one obtains the results plotted in Fig. 11, where the movements of the middle of the spans are shown both for the stiff and for slender pylons. From these results, the influence of the rigidity of the pylons can be clearly observed.

In the plots of Fig. 12, one can observe the deformed shape of the bridge deck at different instants of the pylons' movement both for the stiff and slender pylons. Finally, in Fig. 13 the tensions of the cables at different instants of the pylons' movement are also shown. For both pylons with equal motions, the bridge distress is higher, while for pylons with different motions (due to different soil properties), the bridge distress is lower. Thus, the stiffness of the pylons reduces dramatically the seismic action and its influence on the bridge.

6.2 Two pylons with different oscillations

Let us consider now that each pylon oscillates differently according to the following equations

$$e_a = 0.03 \cdot e^{-0.5 \cdot t} \mathrm{Sin}(8 \cdot t), \quad e_b = 0.02 \cdot e^{-0.5 \cdot t} \mathrm{Sin}(8 \cdot t + 1) \tag{22}$$

as shown in Fig. 14.

By applying the formulae of §4 and 5, one gets the results plotted in Fig. 15, where the movements of the middle of the spans are shown both for the stiff and for slender pylons. The

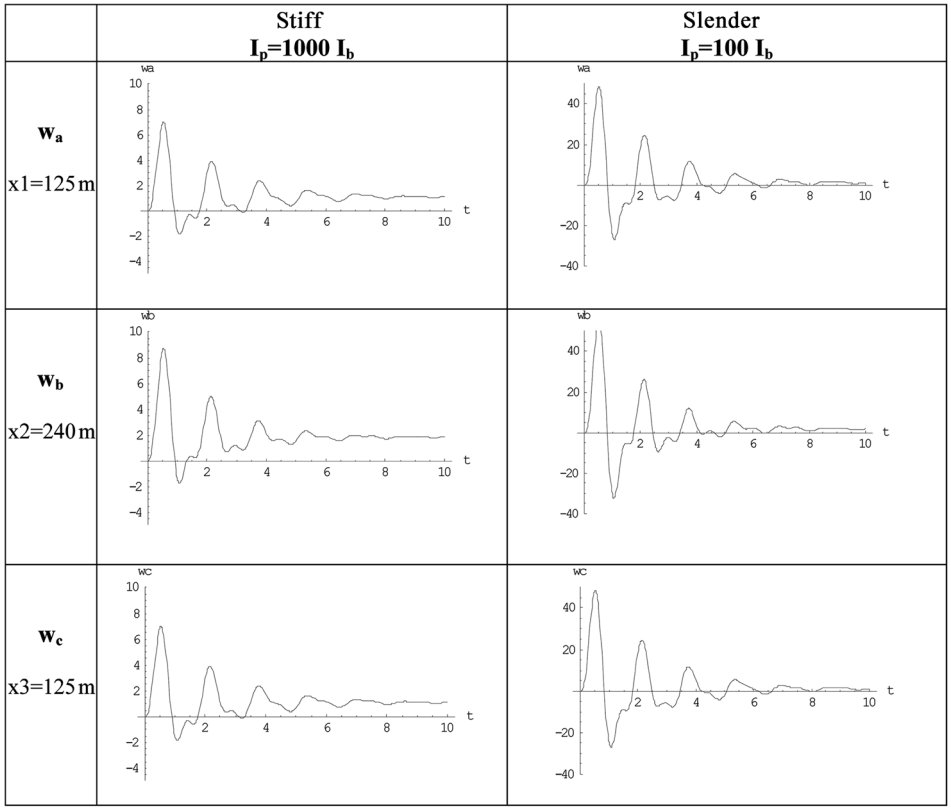

Fig. 11 Dynamic displacements at midspan for stiff and slender pylons

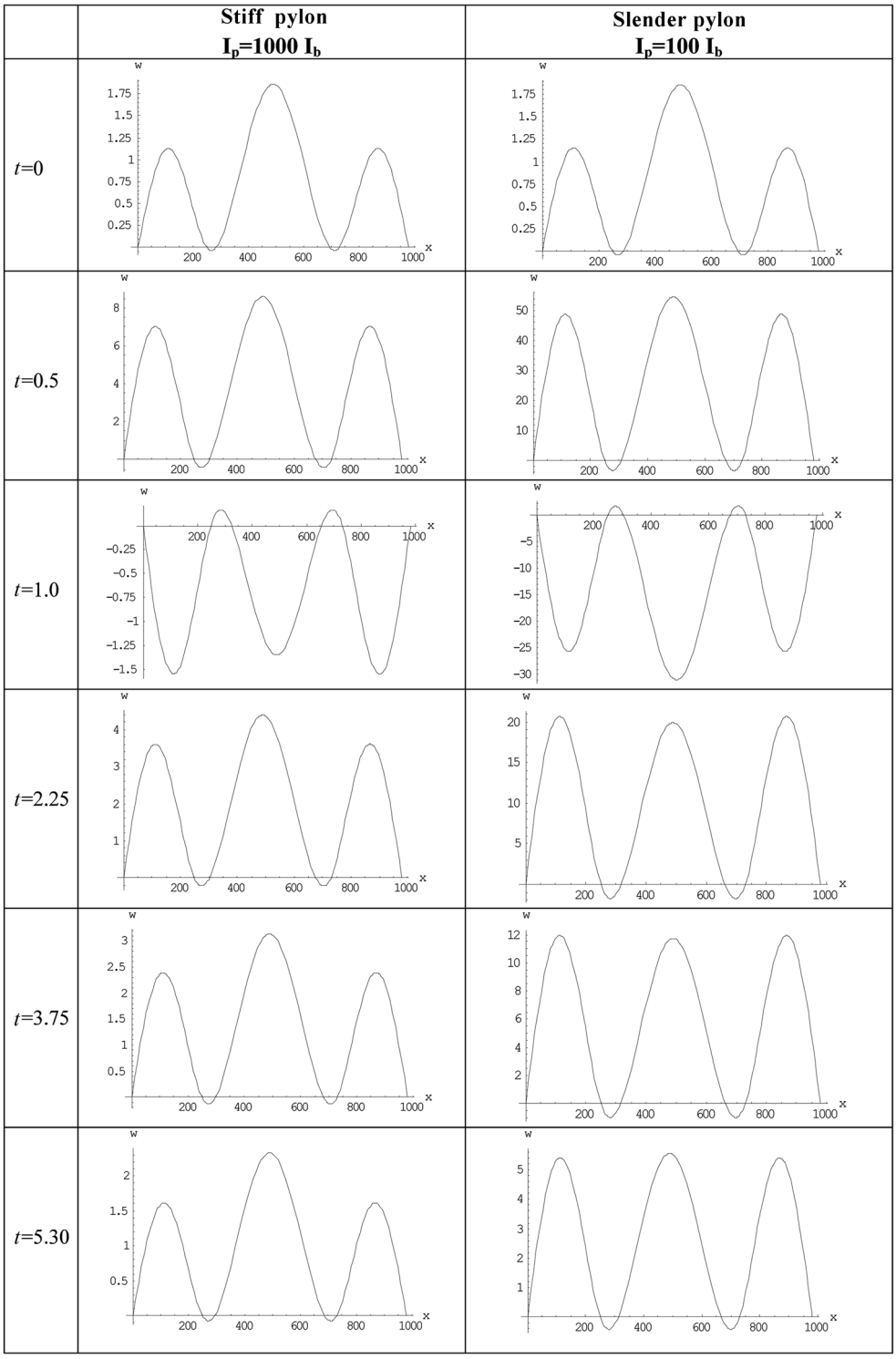

Fig. 12 The deformed shape of the bridge deck at different instants of the pylons' movement

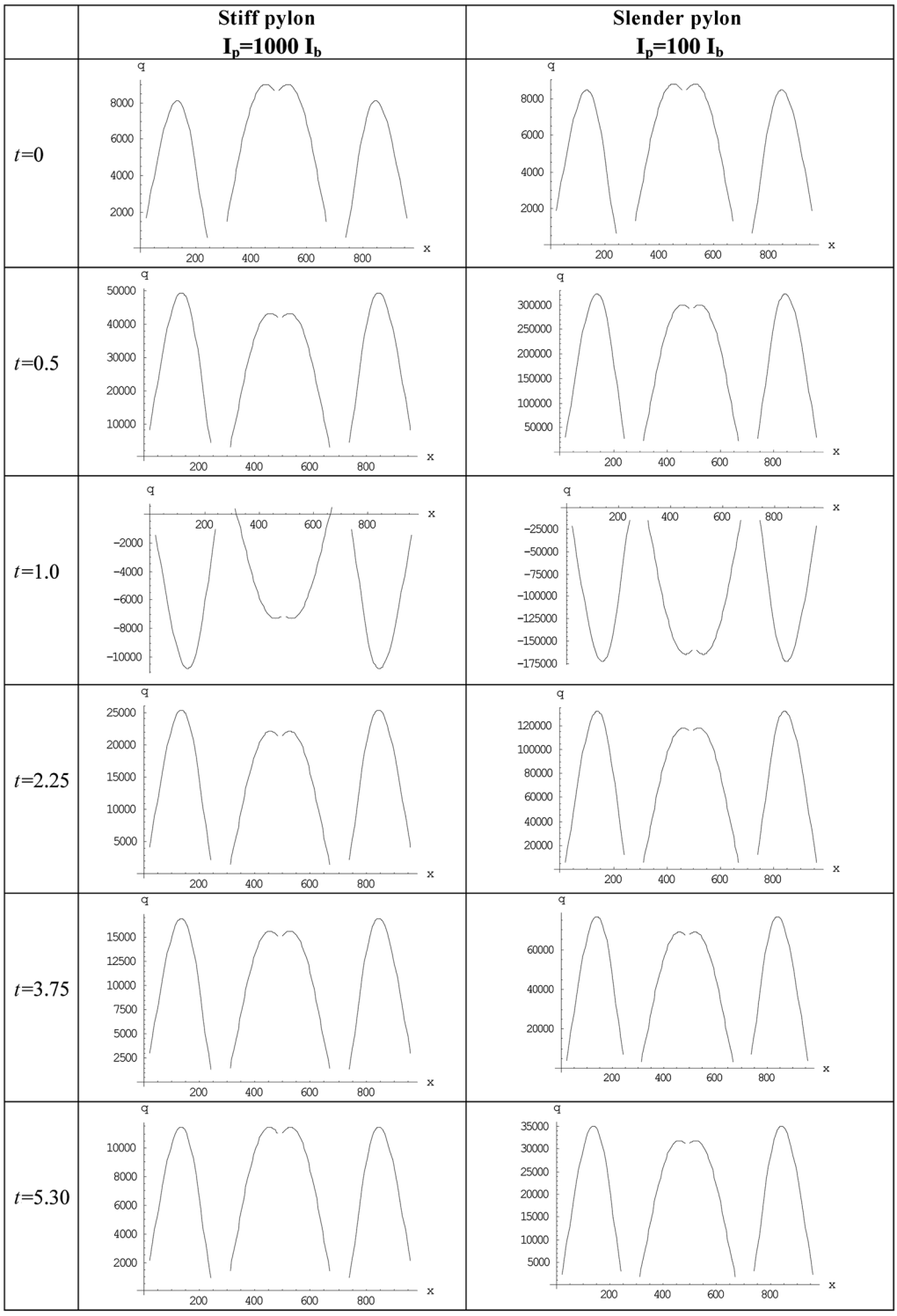

Fig. 13 The tensile forces of the cables at different instants

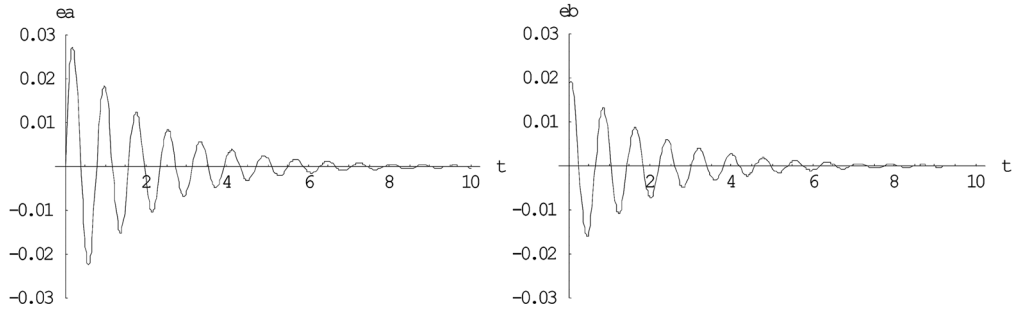

Fig. 14 Oscillations of two pylons

	Stiff pylon $I_p=1000\ I_b$	**Slender pylon** $I_p=100\ I_b$
w_a x1=125 m	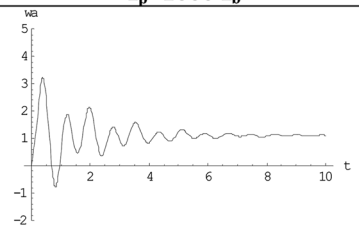	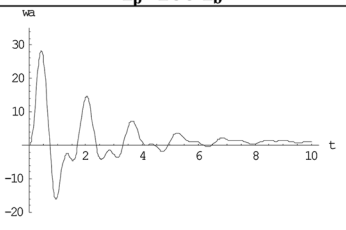
w_b x2=240 m	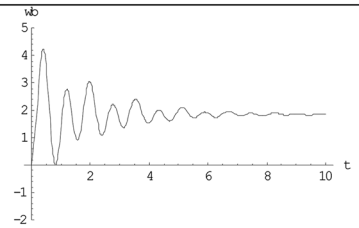	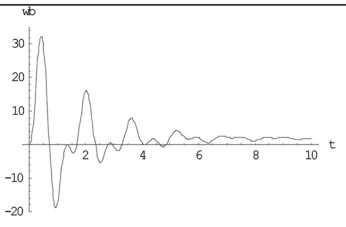
w_c x3=125 m	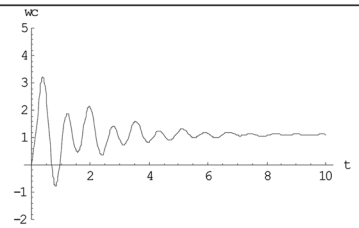	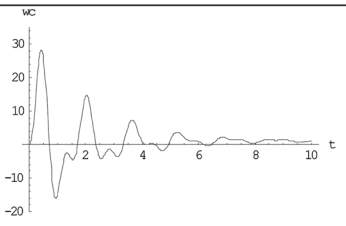

Fig. 15 Dynamic displacements at midspan for stiff and slender pylons

vertical motion of the pylons is significant when they are located at a distance that is less than 0.8 to 1.0 times of the earthquake's focus depth. Again, the influence of the rigidity of the pylons can be clearly observed.

In the plots of Fig. 16, the deformed shape of the bridge deck is shown at different instants of the pylons' movement both for the stiff and slender pylons, each moving differently.

Finally, in Fig. 17 the tensions of the cables are shown at different instants of the pylons' movement for pylons with different motions.

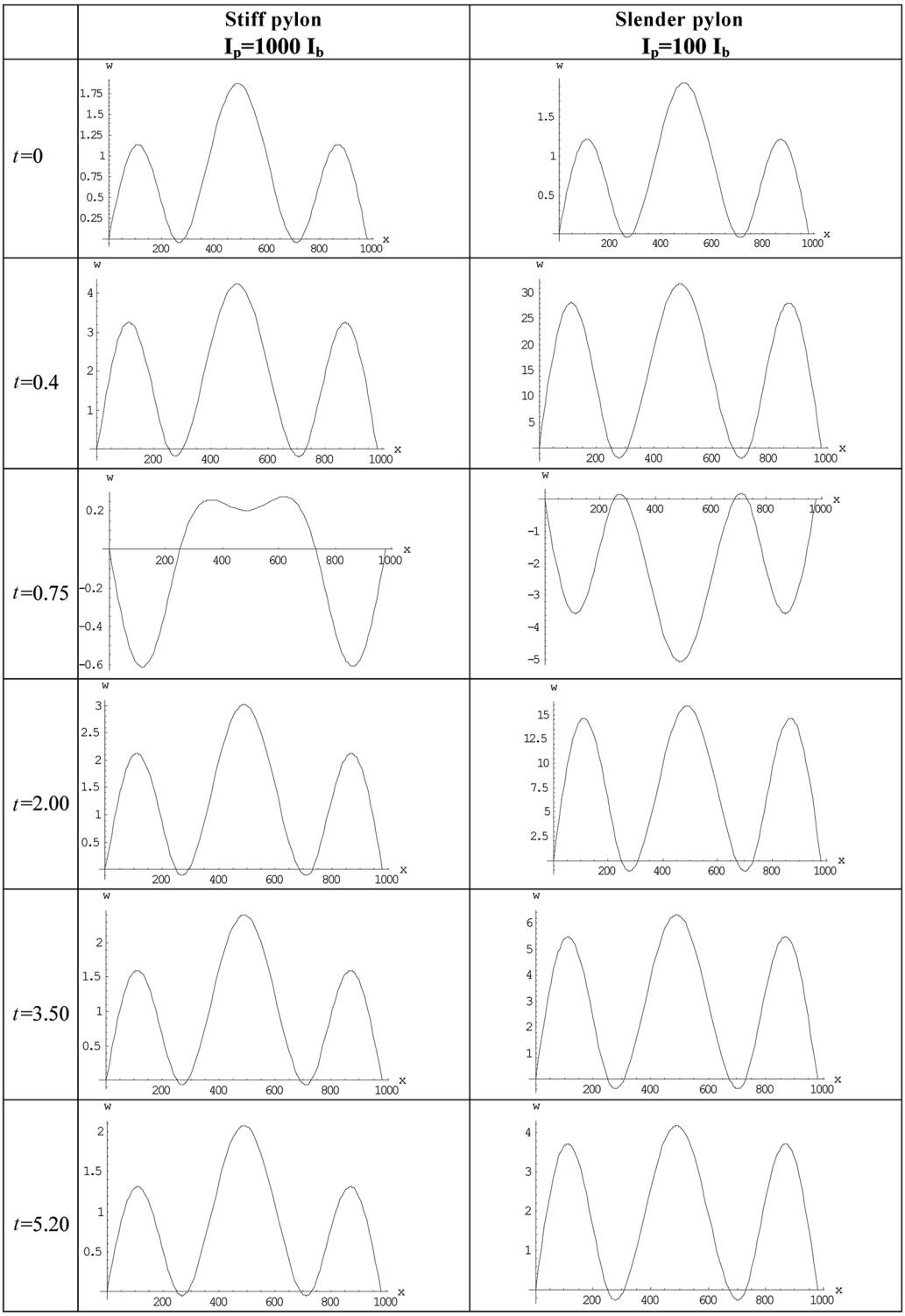

Fig. 16 The deformed shape of the bridge deck at different instants of the pylons' movement

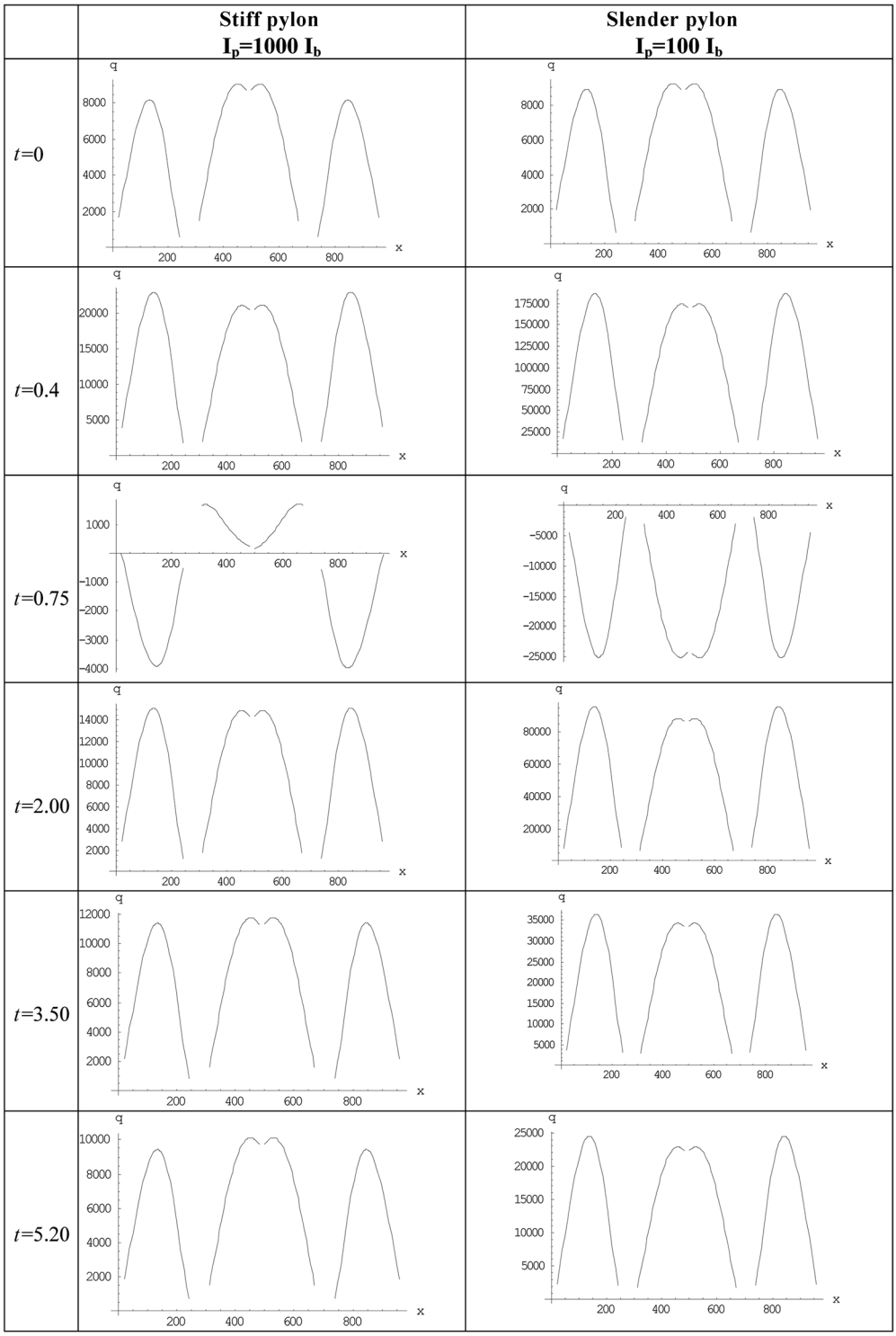

Fig. 17 The tensions of the cables at various time instants

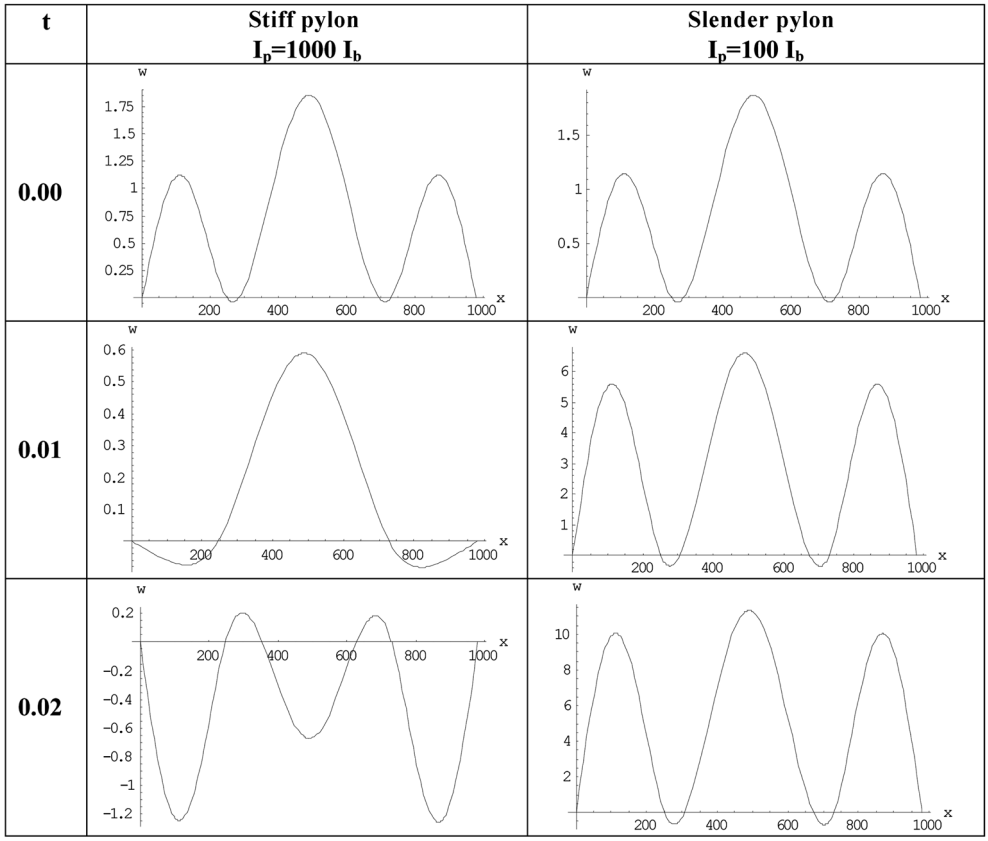

Fig. 18 Deformations of the bridge-deck

6.3 One pylon with permanent subsidence

By applying the formulae for the case with only one pylon undergoing permanent subsidence and for both the stiff and slender pylons, one obtains the results plotted in Fig. 18 for the deck deformations and those in Fig. 19 for the tensions of the cables. From these figures one can see that for stiff pylons, the bridge deck oscillates in a quite different manner and suffers severe negative moments in comparison to the case of slender pylons, while the majority of the tension cables is relieved. The instantaneous developed deck deformations and cable tensions, mainly at the beginning of the seismic action, are significantly greater and in the case of slender pylons they may lead to collapse and disaster. Also, the cables may become non-active, i.e., with negative values or no pulling action on the deck.

6.4 Both pylons with permanent subsidence

By applying the formulae for the case of both pylons undergoing permanent subsidence for both the stiff and slender pylons, one obtains the results plotted in Fig. 20 for the deck deformations and those in Fig. 21 for the tensions of the cables. A comparison of the results shown in these figures

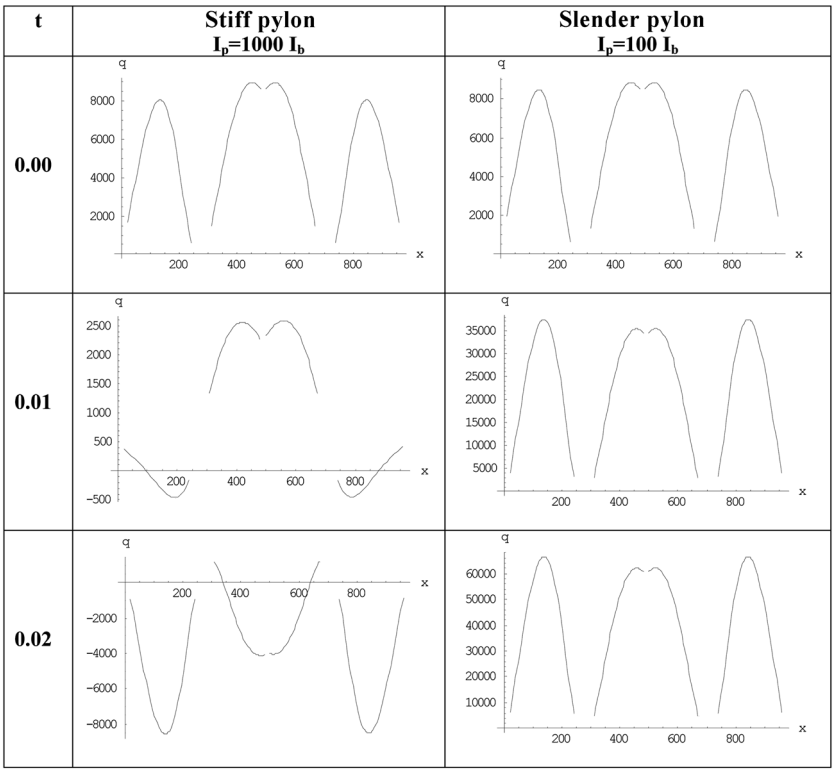

Fig. 19 Tensions of the cables

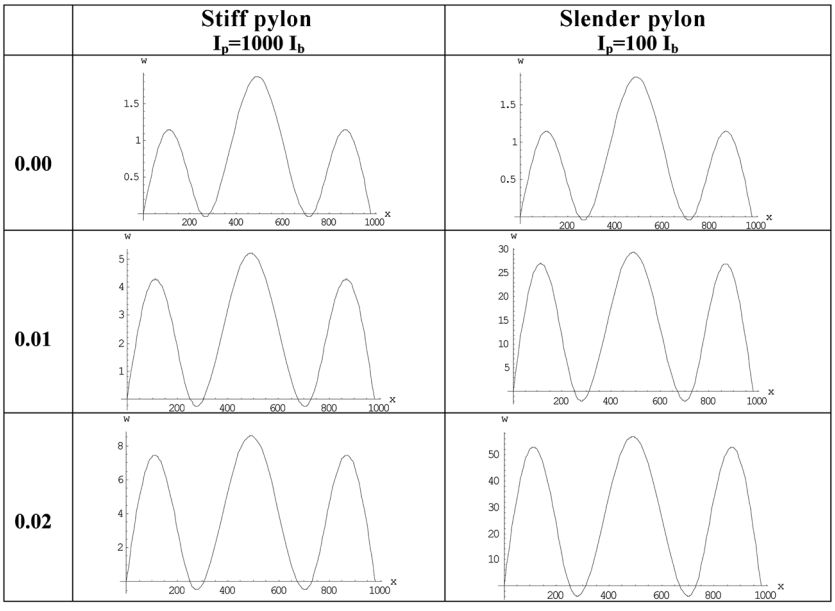

Fig. 20 Deformations of the bridge-deck

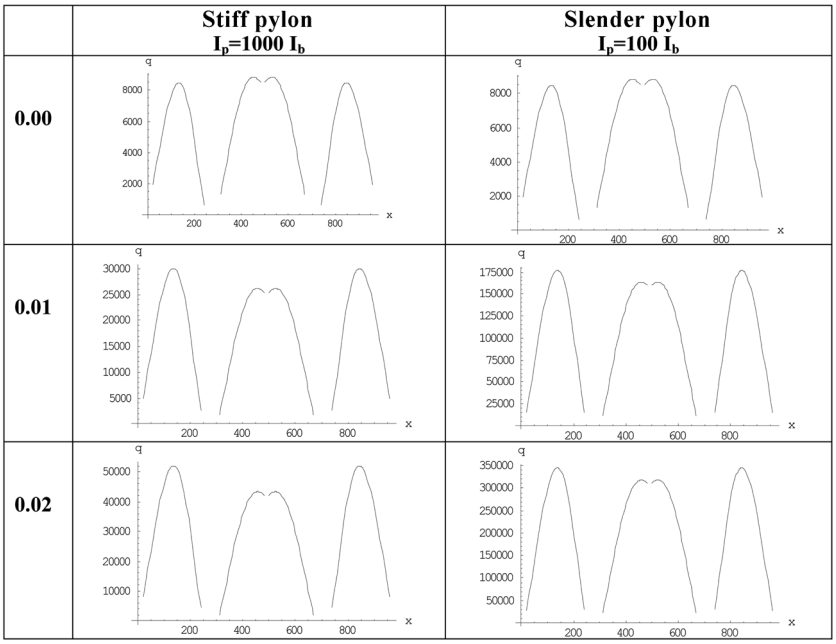

Fig. 21 Tensions of the cables

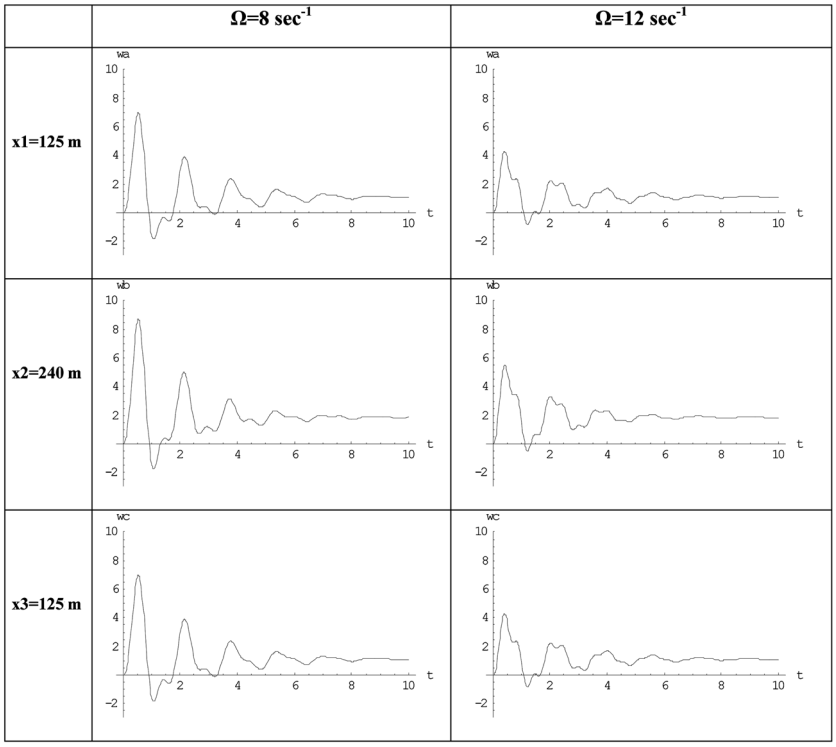

Fig. 22 The influence of the earthquake frequency

with the ones in Figs. 18 and 19 shows that if both pylons subside permanently, the bridge deck deformations are quite similar, but higher for slender pylons, and the same holds true for the tension cables in contrast to the case of a single pylon subsidence.

6.5 Influence of earthquake frequencies

In this paragraph, the influence of the earthquake frequency on the bridge motion is studied for the case of stiff pylons with the same motion according to Eq. (23)

$$e_a = e_b = 0.03 \cdot e^{-0.5 \cdot t} \mathrm{Sin}(8 \cdot t), \quad e_a = e_b = 0.03 \cdot e^{-0.5 \cdot t} \mathrm{Sin}(12 \cdot t) \tag{23}$$

From the results plotted in Fig. 22, one observes that the influence of earthquake frequency is generally significant. Specifically, if the earthquake frequency is increased by 50%, the amplitude of the bridge deck motion drops by 60-70%. It should be pointed out that the seismic frequencies are usually higher than $10\,\mathrm{sec}^{-1}$. Frequencies with values less than $10\,\mathrm{sec}^{-1}$ bring about much bigger deformations and cable tensions.

7. Conclusions

On the basis of the representative cable-stayed bridge models considered and the analyses performed in this paper, the following conclusions can be drawn:

- A simple and efficient model for preliminary study of the cable-stayed bridges subjected to different cases of loadings and pylons' motion is presented herein.
- The vertical motion of the pylons is significant when they are located at a distance that is less than 0.8 to 1.0 times of the earthquake's focus depth. Thus, it is rather an unusual case to consider in engineering practice. Nevertheless, one must examine the consequence of these loadings because of their catastrophic effect.
- An important (but expected) conclusion is the significant influence of the pylons' stiffness on both the deck deformations and tensions of the cables. This stiffness reduces dramatically the seismic action and its influence on the bridge.
- The seismic frequencies are usually higher than $10\,\mathrm{sec}^{-1}$. Frequencies with values less than this bring about much bigger deformations and cable tensions.
- The instantaneous developed deck deformations and cable tensions, mainly at the beginning of the seismic action, are significantly greater and in the case of slender pylons they may lead to collapse and disaster.
- At some instants, mainly at the beginning of the seismic action, the cables may become non-active, i.e., with negative values or no pulling action on the deck.
- For both pylons with equal motions, the bridge distress is higher, while for pylons with different motions (due to different soil properties), the bridge distress is lower.
- For the case with only one pylon undergoing permanent subsidence, the deformations and cable tensions developed are higher. Therefore, the pylons must be designed with the possible greater stiffness.

References

Abdel-Ghaffar, A.M. and Khalifa, M.A. (1991), "Importance of cable vibration in dynamics of cable-stayed bridges", *J. Eng. Mech.-ASCE*, **117**(11), 2571-2589.

Achkire, Y. and Preumont, A. (1996), "Active tendon control of cable-stayed bridges", *J. Earthq. Eng. Struct. D.*, **25**(6), 585-597.

Bosdogianni, A. and Olivari, D. (1997), "Wind-reduced and rain-induced oscillations of cable-stayed bridges", *J. Wind Eng. Ind. Aerod.*, **64**(2-3), 171-185.

Bruno, D. and Grimaldi, A. (1985), "Non-linear behavior of long-span cable-stayed bridges", *Meccanica J.*, **20**(4), 303-313.

Bruno, D. and Golotti, V. (1994), "Vibration analysis of cable-stayed bridges", *J. Struct. Eng. Int.*, **4**(1), 23-28.

Chatterjee, P.K., Datta, T.K. and Suruna, C.S. (1994), "Vibration of cable-stayed bridges under moving vehicles", *J. Struct. Eng. Int.*, **4**(2), 116-121.

Ermopoulos, J., Vlahinos, A. and Wang, Y.C. (1992), "Stability analysis of cable-stayed bridges", *Comput. Struct.*, **44**(5), 1083-1089.

Fleming, J.F. (1979), "Non-linear static analysis of cable-stayed bridge structures", *Comput. Struct.*, **10**(4), 986-1000.

Fleming, J.F. and Egeseli, E.A. (1980), "Dynamic behavior of a cable-stayed bridge", *Earthq. Eng. Struct. D.*, **8**(1), 1-16.

Freire, A.M.S., Negräo, J.H.O. and Lopez, A.V. (2006), "Geometrical non-linearities on the static analysis of highly flexible steel cable-stayed bridges", *Comput. Struct.*, **84**(31-32), 2128-2140.

Gimsing, N. (1997), *Cable supported bridges – Concept and design*, 2nd Edition, John Wiley & Sons, Chichester.

Khalil, M.S. (1999), "Non-linear analysis of cable-stayed bridges at ultimate load level", *Can. J. Civil Eng.*, **23**(5), 1111-1117.

Kollbruner, C.F., Hajdin, N. and Stipanic, B. (1980), *Contribution to the analysis of cable-stayed Bridges*, Inst. For Engineering Research Editions, N.48, Schulthess Verlag, Zürich.

Konstantakopoulos, T.G., Michaltsos, G.T. and Sophianopoulos, D.S. (2002), *A simplified model for the study of the lateral-torsional vibration of cable-stayed bridges - Eurodyn 2002*, Springer, Munich.

Leonard, F. (1972), *Bridges*, Architectural Press, London.

Michaltsos, G.T. (2001), "A simplified model for the dynamic analysis of cable-stayed bridges", *Facta Universitatis*, **3**(11), 185-204.

Michaltsos, G.T., Ermopoulos, J.C. and Konstantakopoulos, T.G. (2003), "Preliminary design of cable-stayed bridges for vertical static loads", *J. Struct. Eng. Mech.*, **16**(1), 1-15.

Michaltsos, G.T. (2005), "Stability of a cable-stayed bridge's pylon, under time-depended loading", Collection of papers in memory of Academician P.S. Theocharis. Inst. of Mechanics Problems and Academy of Sciences, Russia, Inst. Of Mechanics of Nat. Acad. of Sciences, Armenia.

Michaltsos, G.T., Raftoyiannis, I.G. and Konstantakopoulos, T.G. (2008), "Dynamic stability of cable-stayed bridge pylons", *Int. J. Struct. Stabil. Dyn.*, **8**(4), 627-643.

Michaltsos, G.T. and Raftoyiannis, I.G. (2009), "The influence of different support movements and heights of piers on the dynamic behavior of bridges. Part I: Earthquake acting transversely to the Deck", *Interact. Multiscale Mech.*, **2**(4), 431-454.

Michaltsos, G.T. and Raftoyiannis, I.G. (2012), *Bridges' dynamics*, (e-book) Bentham Publ. UAE

Mozos, C.M. and Aparicio, A.C. (2010), "Parametric study on the dynamic response of cable-stayed bridges to the sudden failure of a stay. Part I: Bending moment acting on the deck", *Eng. Struct.*, **32**(10), 3288-3300.

Nazmy, A.S. and Abdel-Ghaffar, A.M. (1990), "Non-linear earthquake response analysis of long-span cable-stayed bridges", *Earthq. Eng. Struct. D.*, **19**(1), 45-62.

Raftoyiannis, I.G., Konstantakopoulos, T.G. and Michaltsos, G.T. (2010), "The influence of different support movements and heights of piers on the dynamic behavior of bridges. Part II: Earthquake acting along the Bridge Axis", *Interact. Multiscale Mech.*, **3**(1), 39-54.

Raftoyiannis, I.G., Michaltsos, G.T. and Konstantakopoulos, T.G. (2012), "Behavior of cable-stayed bridges built over faults", *Interact. Multiscale Mech.*, **5**(3), 187-210.

Troitsky, M.C. (1988), *Cable-stayed bridges – Theory and design*, 2nd edition, B.S.P. Professional Books,

London.
Virgoreux, M. (1999), "Recent evolution on cable-stayed bridges", *J. Eng. Struct.*, **21**(8), 737-755.
Wang, P.H., Liu, M.Y., Huang, Y.T. and Lin, L.C. (2010), "Influence of lateral motion of cable-stayed bridges", *Struct. Eng. Mech.*, **34**(6), 719-738.